PHYSICAL REVIEW B VOLUME 47, NUMBER 21 1 JUNE 1993-I

Comparison of results and models of solid-phase epitaxial growth of implanted Si layers induced by electron- and ion-beam irradiation

G. Lulli and P. G. Merli
Istituto di Chimica e Tecnologia dei Materiali e Componenti per l'Elettronica del Consiglio Nazionale dell Ricerche, Via Castagnoli 1 - 40126 Bologna, Italy
(Received 13 January 1992; revised manuscript received 20 October 1992)

An outline of new and previously published results of solid-phase epitaxy of implanted Si layers induced below room temperature by electron irradiation in the transmission electron microscope is given. The basic features of the process (i.e., the dependence of epitaxial growth rate on temperature of the target, electron energy, dose rate of irradiation) are discussed and compared with the trends reported in the literature for ion-beam-induced epitaxy obtained in a higher-temperature range (typically $200 \leq T \leq 400\,^{\circ}\mathrm{C}$). The aim is to demonstrate that the fundamental characteristics of electron-beam-induced epitaxy are consistent with the extrapolation to low temperature and low mass of irradiating particles of the features of ion-beam-induced epitaxy, if appropriate assumptions on the kinetics of the defects responsible for the transformation are made. To better clarify this point it is shown that both a purely interface- and a purely diffusion-limited model of particle-induced epitaxy can in principle reproduce the very essential features of the process: the key point being the assumptions made on the dominant mechanism of defect reaction. In fact, while a linear-recombination scheme seems appropriate to explain the results of electron-induced epitaxy below room temperature, a dominant bimolecular-reaction mechanism seems necessary to reproduce the essential features of ion-induced epitaxy. Possible influences on electron-beam-induced epitaxy of electronic excitation or elastic collisions under the threshold for production of Frenkel pairs are also qualitatively discussed.

I. INTRODUCTION

The ability of ion or electron beams to induce epitaxial crystallization of amorphous implanted layers of Si and Ge at temperatures much lower than the value necessary to observe epitaxy with thermal annealing, has been known for several years.[1–5] The renewed interest in this subject during the last few years[6,7] is due to the possibilities of application of low-temperature beam-induced processes in the field of microelectronics. In fact, it seems interesting to optimize the conditions of beam-induced processes in order to improve specific properties of electronic materials which cannot be achieved by simple thermal annealing. The exploitation of such possibilities requires a good comprehension of the basic physical mechanisms governing beam-induced transformations.

As far as radiation-induced solid-phase epitaxy (SPE) of implanted Si is concerned, it has been attempted to formulate qualitative models of the phenomenon, since its early experimental observation.[3] The first aim was to identify by what mechanism the irradiating particles supply the energy necessary to activate the transformation. Even though some authors have suggested that electronic stopping could be responsible for the effect,[4] the prevailing hypothesis is that the energy for the transformation comes basically from the energy deposited in elastic collisions.[3,6,7] This conclusion has been supported by experiments performed on amorphous Si layers which have shown a proportionality of the epitaxial growth rate to the nuclear energy loss of ions,[8] or to the elastic displacement cross section of electrons.[9]

The commonly accepted hypothesis is that the transformation is mediated by defects produced by elastic collisions just at the amorphous-crystalline (a-c) interface[10] or, alternatively, in the bulk (amorphous and/or crystalline material) from where they can diffuse to the a-c interface.[9,11]

The increasing amount of experimental data about the dependence of the growth rate of ion-beam-induced epitaxial crystallization (IBIEC) on the various irradiation and target parameters (dose rate,[7,12,13] substrate orientation,[14] and doping[15,16]) and the observation of the transition to layer-by-layer amorphization, which occurs under ion-beam irradiation when the temperature is reduced below a critical value depending on the dose rate,[17] have stimulated the formulation of models which could account for the observed behaviors.[16,18–22]

Most of the work about beam-induced SPE has been performed on IBIEC (for a recent review of the subject see Ref. 23). Relatively little work has been done, in comparison, on electron-beam-induced epitaxial crystallization (EBIEC).[2,9,16,24–26] The interest in EBIEC experiments is related to the possibility of using beam energies both below and above the threshold for defect production E_d ($E_d \simeq 145$ keV for Si,[27] corresponding to a threshold $T_d \simeq 13$ eV in the kinetic energy transferred to the recoil) and of exploring a range where the quantitative aspects of the stopping processes are much different from the case of ions, due to the large difference in the mass of irradiating particles.

The stopping characteristics of electrons in Si are summarized in Fig. 1, where the displacement cross section σ_d of electrons in Si, which was calculated[28] by assuming $T_d = 13$ eV, and the electronic (inelastic) stopping for electrons, in an energy range typical of transmission electron microscope (TEM), are reported.

 ©1993 The American Physical Society

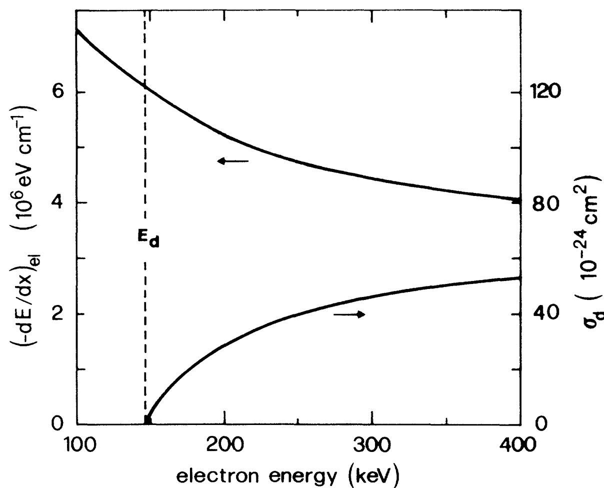

FIG. 1. Inelastic energy loss (left scale) and elastic displacement cross section (right scale) of electrons in Si as a function of electron energy. Displacement cross section is calculated according to Ref. 28 by assuming a displacement threshold of the energy transferred in elastic collisions $T_d = 13$ eV. $E_d \simeq 145$ keV is the corresponding threshold for the incident electron energy.

In this work we present new results and review previously obtained ones of EBIEC performed at temperature $T \leq 20\,°C$. Analogies and differences with the results of IBIEC reported in the literature are pointed out and discussed.

II. EXPERIMENT

Si wafers (001)-oriented, Cz-grown, *p*-type, with a resistivity of about 1 Ω cm, were implanted at room temperature with 100-keV Si^+ ions at a dose of 2×10^{15} ions cm^{-2}. This implantation condition produced a surface amorphous layer about 210-nm thick. Thin cross sections for TEM were prepared by mechanical thinning and ion milling.

The irradiations were performed mainly on a Philips CM-30 TEM, equipped with a LaB_6 cathode and a liquid-helium cool stage, capable of operating at temperatures in the range $-258 \leq T \leq 20\,°C$. The irradiations were performed with a beam spot having a radius of about 1 μm, centered at the *a*-*c* interface on cross sections ⟨110⟩ aligned. The reported results will refer to beam energies of 100, 175, 200, and 300 keV. The current density J varies in a range $60 \leq J \leq 600$ A cm^{-2}. The chosen values of irradiation temperature are -258, -170, -140, -120, -100, and 20 °C.

The typical duration of a single growth experiment is between 1 and 2 h for $J \simeq 100$ A cm^{-2}. The current density from which the irradiation dose is calculated, is monitored every 5 or 10 min by means of a Faraday cage, adjustable in position, inserted in the observation chamber of the microscope, following a procedure analogous to the one described in Ref. 9. A picture of the irradiated region is recorded every time after the measurement of J.

Each experimental point of the rate of beam-induced SPE is an average of several measurements. The bars reported in the graphs represent casual errors due to the fluctuations in the current density, the errors in the measurements of the epitaxially grown layer, and the spread in the results of the various irradiations performed at the same nominal conditions. A systematic error of 20%, which has been estimated to affect the current-density (and, as a consequence, the dose) measurement, has not been reported, since we are interested in the behavior of the SPE rate as a function of irradiation parameters, rather than in its absolute values.

A theoretical estimation of the beam-heating effect has been made in Ref. 9 in order to demonstrate that the irradiated spot remains practically at the same temperature of the specimen holder. The theoretical expression[29] indicates that the temperature increase due to beam heating is proportional to the current density in the spot. As a consequence, the experimental observation that the growth per unit electron dose is strictly independent of the beam current density under the whole range of irradiation parameters investigated, leads automatically to exclude the occurrence of beam-heating effects.

A proper question is if the growth observed on thin cross sections is representative of the behavior of a bulk material, i.e., if "thin-film" effects do not perturb EBIEC. It has been shown[30] how the thermal SPE induced on cross sections of implanted Si samples by heating them *in situ* under TEM observation, is retarded if the specimen thickness is less than about 20 nm.

Figure 2 is a TEM image of a cross section of implanted Si, in a region where the specimen thickness decreases going from the left to the right of the picture, which has been heated *in situ* at $T \simeq 540\,°C$. The above-mentioned effect is clearly demonstrated, as a decreasing SPE rate which occurs when the specimen thickness is reduced below a critical value estimated to be some tenths of nm. The saturation value of the SPE rate (about 5.5 nm s^{-1}) measured in the left region of Fig. 2, is equal to the rate observed in bulk samples annealed in a furnace at the same temperature. An analogous effect of retardation has been observed during EBIEC experiments when irradiating specimen regions of thickness less than some tenths of nm. For this reason all irradiations were performed in regions of thickness >150 nm, where no dependence of the measured SPE rate on specimen thick-

FIG. 2. TEM bright-field image of a cross section of self-implanted Si during heating *in situ* at 540 °C. The arrow indicates the direction along which the thickness of the specimen decreases. (a) amorphous layer, (c) epitaxially grown crystalline layer, (b) bulk crystal. The effect of the reduced SPE rate in the thinner region is evident.

ness is observed. For analogy with the thermal experiments the SPE rate measured under such conditions has been considered to represent the behavior of the bulk material.

III. RESULTS

A. Temperature and energy dependence of the EBIEC rate

Figure 3 is an Arrhenius plot in which the thickness of the epitaxially grown layer per unit electron dose is reported as a function of temperature, for the different electron energies used in the irradiations.

Irradiations have also been performed at electron energy of 100 keV: the result is that no growth occurs even for very long irradiation times.

The data in the interval $-170 \leq T \leq 20$°C can be described by very small apparent activation energies (about $0.4-0.9 \times 10^{-2}$ eV), tending to decrease when lowering electron energy. However, the results at $T = -258$ °C cannot be obtained by the extrapolation of these data. In fact, with decreasing T the apparent activation energy still decreases down to a practically negligible value.

Figure 4 reports the data of Fig. 3 as a function of electron energy for the different irradiation temperatures. The linear scale has been introduced in order to make more evident the effect of the reduction in the dependence of the growth rate on T with decreasing electron energy.

Figure 5 reports the growth rates normalized to the value measured for an electron energy of 300 keV at the different temperatures of irradiation, as a function of electron energy. The full lines represent the normalized displacement cross section σ_d, obtained with the McKinley and Feshbach approximation to the exact Mott scattering formula.[28] Each curve is calculated for a different value of the atomic displacement threshold T_d. The results are consistent with the hypothesis of a growth rate proportional to the displacement cross section if a threshold $12 \leq T_d \leq 14$ eV, is assumed, which is the range most widely accepted in the literature[27] and theoretically confirmed by molecular-dynamics simulations.[31]

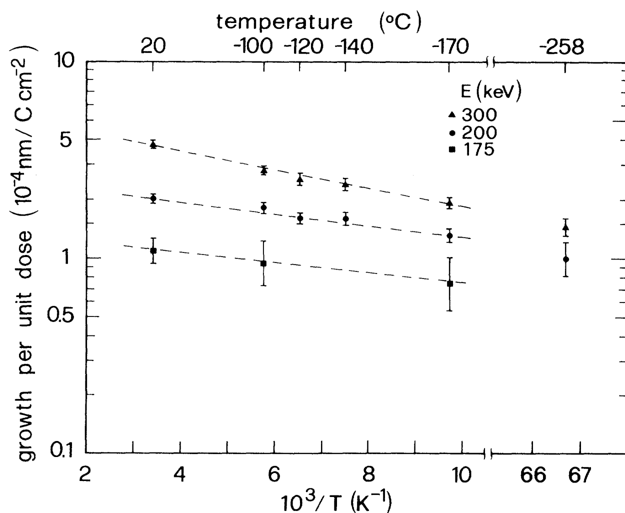

FIG. 3. Arrhenius plot of the thickness of the epitaxially grown layer per unit dose reported as a function of temperature, for the different electron energies used in the irradiations. The dashed lines are drawn as a guide to the eye.

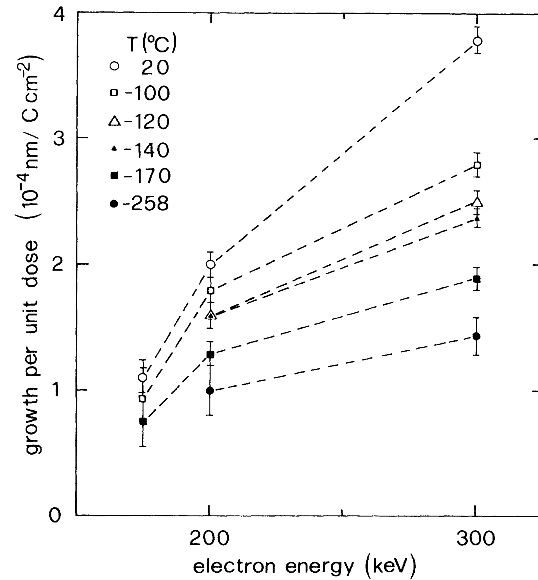

FIG. 4. The same data of Fig. 3 reported on a linear scale as a function of electron energy, for the different irradiation temperatures.

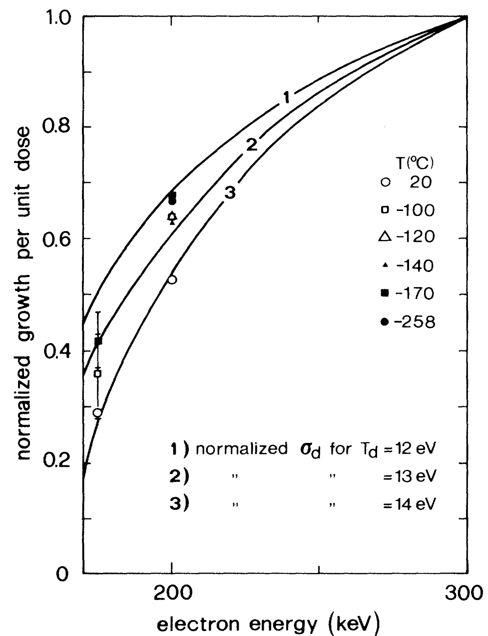

FIG. 5. EBIEC rates normalized to the maximum values observed for electron energy of 300 keV as a function of electron energy for the different temperatures of irradiation. Full lines represent the displacement cross sections, calculated for three different values of the threshold energy T_d, normalized to the value at $E = 300$ eV.

It is interesting to point out that TEM observations, using diffraction contrast mode, as well as high-resolution electron microscopy (HREM) techniques, indicate that in EBIEC there are not strongly preferred sites for the crystallization of atoms at the *a-c* interface.

Figure 6 is an example of a HREM image of a sample in (110) projection before and after irradiation with 300-keV electrons in an Hitachi 9000 TEM for a time of 28 min at room temperature. It gives just a qualitative picture of the process, due to the absence of a Faraday cage for the measurement of the irradiation dose. The dotted line in (b) indicates the position of the original *a-c* interface. It is interesting to observe how the original undulations in the *a-c* interface show no tendency to smooth out, as instead occurs during thermally induced SPE of (001) Si samples amorphized by Si^+ implantation.[32] The layer marked in Fig. 6(b) is too thin to be structurally characterized in detail. This is due to the slow growth which can be obtained on very thin cross sections (necessary for high-resolution imaging), which is a consequence of the above mentioned "thickness" effect. Localized electron-diffraction patterns obtained on thicker samples, where growth is of the order of 100 nm,[9] clearly show the crystalline nature of the grown layer in spite of a large amount of small unresolved defects. Moreover rodlike defects, a well-known consequence of electron irradiation at $E > E_d$, are clearly visible.

B. Influence of doping on EBIEC

We do not report here the previously published results which refer to irradiation of amorphous layers doped with P, As, and B.[16] We just recall that the maximum difference in EBIEC rates observed on doped and undoped samples was less than a factor of 2, pointing out a doping dependence much weaker than the one observed in thermal SPE. In considering this result one should take into account also the effect, quite difficult to quantify, of charge injection due to electronic excitation by the irradiating beam. A strong injection condition should, in fact, shift the position of the Fermi level in doped crystalline Si towards the midgap, reducing the difference in its electrical behavior with undoped Si. A similar argument could for instance suggest an explanation of the results of combined effect of doping level and dose rate on the growth rate of crystalline Si grains irradiated by Xe^+ ions, reported in Ref. 33.

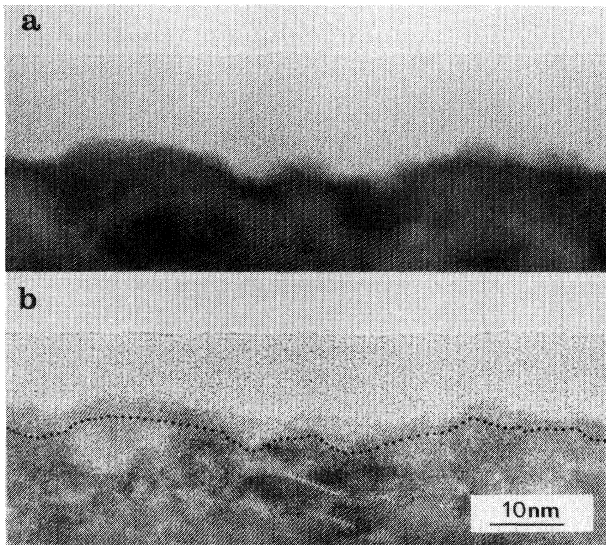

FIG. 6. High-resolution electron microscopy (HREM) image of a thin region of a self-implanted Si sample in (110) projection, before (a) and after (b) irradiation with 300-keV electrons for a time of 28 min at room temperature. The dotted line in (b) indicates the position of the original *a-c* interface.

C. Summary of results

We synthesize here the most relevant results of EBIEC experiments in some points which we will refer to in the forthcoming section to discuss analogies and differences with IBIEC.

(i) EBIEC takes place down to temperature of about 15 K; no transition to layer-by-layer amorphization is observed.

(ii) The temperature dependence of the growth rate is very weak in the range investigated. The apparent activation energies observed in the range $-170 \leq T \leq 20\,°C$ are 1–2 orders of magnitude lower than the typical values characteristic of defect migration[34] and show a tendency to decrease with decreasing temperature and electron energy.

The two points above indicate that the EBIEC rate (in terms of growth per unit time) is proportional to the defect production rate G, which can be written as $G = J\sigma_d/e$, where e is the electron charge.

(iii) The EBIEC rate scales linearly with the displacement cross section calculated assuming a value for the effective threshold of transferred energy for displacement in the range $12 \leq T_d \leq 14$ eV. No growth is observed for under-threshold irradiation.

(iv) The growth rate per unit electron dose is independent of the beam current density J in a range $60 \leq J \leq 600$ A cm^{-2}.

(v) Weak doping dependence of EBIEC is observed in comparison with thermally activated SPE.

IV. DISCUSSION

A. Comparison of IBIEC and EBIEC experimental results

Analogies of EBIEC and IBIEC are readily identified with respect to points (iii) and (v) of Sec. III C (see Refs. 8, 14, and 15). An important difference is found in point (i). It has been shown in a previous work[24] that the extrapolation to the range of very low damage defect production of the results, which illustrate the relation between the critical temperature for the transition to layer-by-layer amorphization and the quantity (displacements)^2 (dose rate),[13] cannot describe the behavior of EBIEC. In fact, such extrapolation would predict the "reversal" of EBIEC at a temperature of the order of 20 °C, for the typ-

ical energy and dose rate conditions used in the experiments.

By examining the results in Fig. 12 of Ref. 13, it can be seen that the data relative to the lighter ions do not fall exactly on the reported fit. In fact, the experimental critical temperature for them is lower than the one predicted by the extrapolation of the data of heavier ions.

In a recent work,[35] the efficiencies of various ions in promoting IBIEC are examined in a wide range of ion masses. It is concluded that, while for relatively heavy ions the growth per unit dose scales as the square of nuclear stopping (in agreement with the results reported in Ref. 13), for light ions the recrystallization efficiency is higher than the one predicted by such rule.

We can consider the results reported in Refs. 13 and 35 as an indication that the behavior of IBIEC induced by light ions deviates from the behavior observed for heavy ions in a direction consistent with the results of EBIEC experiments.

As far as point (ii) is concerned, it is not possible to make here a direct comparison between IBIEC and EBIEC, because for T below room temperature ion irradiation generally induces amorphization. Anyhow, we can resort to the results of EBIEC experiments performed by other authors in the typical temperature range of IBIEC ($200 \leq T \leq 400\,^{\circ}\mathrm{C}$),[25] in which they measure an apparent activation energy of the same order as the one observed for IBIEC.

Point (iv) is in general not true for ions. IBIEC, in fact, depends on dose rate, the growth per unit dose being lower for higher dose rates. Nevertheless it is observed that such dependence becomes less pronounced when decreasing ion mass and/or temperature.[12,13]

According to the above observations it can be concluded that where a qualitative difference between the two processes exist, it seems to be a simple consequence either of the different mass of particles involved or of the temperature ranges to which the results refer.

In the light of this conclusion we may investigate what are the specific physical assumptions that need to be modified, when applying to IBIEC and EBIEC the same model of beam-induced SPE, in order to reproduce such differences.

B. Survey of the approaches to the description of beam-induced SPE

The natural starting point for elaborating a model of radiation-induced SPE, is the expression used to describe the transformation at thermal equilibrium. The SPE rate v can be written as

$$v=\lambda \nu f X\left[1-\exp\left[-\frac{\Delta G_{ac}}{kT}\right]\right] , \tag{1}$$

where λ is the lattice spacing, ν is the jump frequency of atoms at the a-c interface, which can be written as $\nu=\nu_0 \exp(-\Delta G_m^*/kT)$, where ν_0 is typically considered to be the Debye frequency and ΔG_m^* the free-energy barrier for an atomic jump, $1/f$ is the number of jumps necessary for one atom to pass from one phase to the other at the a-c interface, X is the atomic fraction at the interface of the sites where an atom from the amorphous phase can be crystallized, ΔG_{ac} is the atomic free-energy difference between the amorphous and the crystalline phase, T the temperature, and k is the Boltzmann constant.

A procedure to write an expression for beam-induced SPE is to retain Eq. (1) and modify properly both X and ΔG_{ac}, in order to take into account the effect of irradiation on the atomic fraction of interface crystallization sites at the interface and on ΔG_{ac}.[18,19] The rate v can become negative (this corresponding to the transition to layer-by-layer amorphization) if the free-energy difference between the two phases at the interface changes its sign as a consequence of irradiation. Other authors consider only the kinetic term out of the square brackets of Eq. (1),[16,20–22] making more or less implicitly the assumption that irradiation does not modify appreciably ΔG_{ac}.[36] In any case the problem is the calculation of X under bombardment.

If in general we consider the possibility that defects responsible of SPE can be created far from the a-c interface, diffuse towards it and recombine there, then a gradient in X is established, which drives the diffusion of defects towards the interface. We can mathematically treat this case by writing a diffusion equation for defects with the appropriate boundary conditions at the a-c interface.

It is interesting to show that, due to its generality, such approach may include both the diffusion- and the interface-limited regimes of transformation as limit cases.

C. Diffusional approach

We will assume that the defects whose concentration is the rate limiting factor of the transformation at the a-c interface are vacancies. Their recombination there with atoms which are not in regular lattice sites is equivalent to these atoms jumping to the proper crystallines positions. Further simplifying assumptions, already made in Ref. 26 are (i) for the process of interest a quasisteady state of defect concentration (i.e., a concentration whose variation in time, both in the long and in the short period, are negligible) is reached in a time small in comparison with the typical irradiation time, and (ii) among the various possible bulk reactions we will consider only the linear recombination of defects at fixed unsaturable centers.

As shown in the following, the latter assumption, although not obvious, is justified from a phenomenological point of view by the behavior of the experimental results. It must be underlined that neglecting direct interstitial-vacancy recombination leads to the equations being identical for the two kinds of defects, so only vacancies need to be considered.

Now we can directly write the equation for vacancy concentration (in units of cm^{-3}) as

$$D_v \frac{d^2 N_v(x)}{dx^2}+G-k_v c_v N_v(x)=0 , \tag{2}$$

where $N_v(x)$ is the spatially dependent concentration of vacancies, D_v is the diffusivity of vacancies, G the num-

ber of stable Frenkel pairs produced per unit volume and time, c_v the bulk concentration of unsaturable recombination centers for vacancies, and k_v the rate coefficient of the linear-recombination process.

Suitable boundary conditions are

$$D_v \left[\frac{dN_v(x)}{dx} \right]_{x=x_{ac}} = sN_v(x_{ac}) , \tag{3}$$

$$D_v \left[\frac{dN_v(x)}{dx} \right]_{x\to\infty} = 0 . \tag{4}$$

In Eq. (3), x_{ac} indicates the position of the *a*-*c* interface, and s is a quantity related to the interfacial defect recombination rate. The relation represents the continuity equation for defects at the *a*-*c* interface, where the term $sN_v(x_{ac})$ is the number of defects recombining per unit time and area, which must be equal to the flux of defects arriving at the interface. Equation (4) indicates that at a large distance from the interface the concentration of vacancies is uniform.

To introduce the reaction mechanism at the interface, expressed by Eq. (1), we can write s as

$$s = \lambda\nu \left[1 - \exp\left[-\frac{\Delta G_{ac}}{kT} \right] \right] . \tag{5}$$

We underline that the introduction of Eq. (3), instead of the condition $N_v(x_{ac})=0$, used in Ref. 26, represents a generalization of the early approach, allowing the consideration of the interface reaction mechanism which was neglected there.

The analytical solution of Eq. (2) at the *a*-*c* interface with the boundary conditions (3) and (4) is

$$N_v(x_{ac}) = \frac{G(L_v^*)^2}{(D_v + L_v^* s)} . \tag{6}$$

In Eq. (6), $L_v^* = \sqrt{D_v/k_v c_v} = \sqrt{1/4\pi r_0 c_v}$, where we have used the relation $k_v = 4\pi r_0 D_v$,[37] in which r_0 is the effective recombination radius of the vacancy sinks. L_v^* may be considered as a typical diffusion length, or average free path of vacancies which, although explicitly independent of T, may depend implicitly on it through r_0.

In Eq. (6) it is possible to identify two limit solutions:

(i) if $s \gg D_v/L_v^*$, then the denominator is $\simeq L_v^* s$ and the rate of transformation v is given by

$$v = \frac{fsN_v(x_{ac})}{N_{\rm Si}} = \frac{fGL_v^*}{N_{\rm Si}} , \tag{7}$$

where $N_{\rm Si}$ is the atomic density of Si. $N_v(x_{ac})/N_{\rm Si}$ is the atomic fraction of vacancies at the interface. This corresponds to the pure diffusion-limited case[16] (i.e., large diffusion length of defects and/or large recombination rate of defects at the *a*-*c* interface);

(ii) if $s \ll D_v/L_v^*$, then the denominator is $\simeq D_v$ and the rate of transformation is given by

$$v = \frac{fsN_v(x_{ac})}{N_{\rm Si}} = \frac{fsG(L_v^*)^2}{N_{\rm Si} D_v} . \tag{8}$$

This corresponds to the pure interface-limited case (see, for instance, Ref. 19) (i.e., small diffusion length of defects and/or small recombination rate at the interface).

The consequence of neglecting both defect clustering and mutual recombination is that the solution $v = fsN_v(x_{ac})/N_{\rm Si}$ depends linearly on G both in the diffusion-limited and in the interface-limited cases. Furthermore, if we assume that $s \propto \exp(-\Delta G_{vm}^*/kT)$ and $D_v \propto \exp(-\Delta G_{vm}^*/kT)$, the exponential term containing the strongest dependence on T through the migration energy ΔG_{vm}^*, disappears also in (8).

If we introduce in Eq. (2) terms describing bimolecular reactions between defects (i.e., clustering or mutual recombination) the solution is no longer analytic. Anyhow, it can be shown[22] that in such case the transformation rate is a nonlinear function of G, and its expression would contain one (or more) exponential terms with ΔG_{vm}^* which would reasonably give a temperature dependence stronger than the one allowed by Eq. (7) or Eq. (8).

D. Application of a recent model of IBIEC to EBIEC

Alternative approaches, based on the assumption that the process is purely interface limited[18–20] and, furthermore, that the defects which mediate the transformation can exist only at the *a*-*c* interface and not far from it,[21] lead to a different procedure for the calculation of X in Eq. (1). Due to its capability of explaining satisfactorily most IBIEC results, we will refer here to a recent model proposed by Jackson,[20] trying to adapt it in order to describe EBIEC. The key assumption of this model in order to explain both temperature and dose rate dependence of IBIEC, is that defects responsible for SPE are created and annihilated in pairs.

In order to explain layer-by-layer amorphization Jackson introduces a quantity V_α which represents the volume of amorphous material created at the interface per unit time by each ion. At the same time the defects left behind by the ions produce a crystallization, whose rate R_x is given by

$$R_x = \frac{a\langle N\rangle\Lambda}{\tau_j} , \tag{9}$$

where a is the lattice parameter, $\langle N\rangle$ is the time-averaged defect density at the interface, Λ is the volume of crystal created by a single defect jump, and $1/\tau_j$ is the frequency of jumps, which can be written as $1/\tau_j = \nu_0 \exp(-E/kT)$ ($\nu_0\sim$ Debye frequency, E = free-energy barrier for atomic jump). The condition $V_\alpha\phi > R_x$, where ϕ is the ion flux, means that amorphization becomes faster than crystallization at the interface, i.e., the transformation is reversed.

This way of treating the balance between amorphization and crystallization allows a straightforward application of the model to EBIEC, for which the assumption $V_\alpha = 0$, can automatically account for the observed lack of transition to layer-by-layer amorphization, even at $T \simeq -258\,^\circ$C. Further peculiarities of EBIEC are (i) the density of defect generation G is calculated as a pure effect of elastic displacements (i.e., no thermal-spike effects, which have been postulated for instance in Ref.

21, are expected for electron irradiation, due to the low-energy transferred in each scattering event), and (ii) the ratio γ of τ_0 (average time between the arrival of particles at the interface) to τ_j is much lower for electron irradiation than for ion irradiation, due to the higher electron current density. The consequence is that, even if the density of defect production (N_0 in the Jackson model) is much lower for electrons in comparison with ions, the defect concentration at the interface will build up in a way similar to that shown in the lower part of Fig. 5 of Ref. 20, reaching a quasistationary value whose fluctuations in time are very small, due to the very small decay of defect concentration expected during the interval τ_0 between the arrival of the ith and the (ith+1) electron.

If we retain the assumption of Jackson about the fact that defects responsible for SPE generate and recombine in pairs, their uniform concentration N will obey

$$\frac{dN}{dt}=2G-k_2N^2 , \tag{10}$$

where k_2 is the rate coefficient of mutual recombination. Equation (10) gives at the quasisteady state

$$\langle N\rangle \simeq N=\sqrt{2G/k_2} . \tag{11}$$

By using the same notation as Ref. 20, and writing $k_2=\sigma^2 a/\tau_j$, where σ^2 is the cross section for mutual recombination, the net crystallization rate becomes from Eq. (9)

$$R_x=\sqrt{2Ga v_0/\sigma^2}\Lambda \exp\left[-\frac{E}{2kT}\right] . \tag{12}$$

The model of Ref. 20 assumes $E=1.2$ eV from the experimental results reported in Ref. 13. So, in accordance with Eq. (12), we should observe a square-root dependence of EBIEC rate on G and an apparent activation energy of 0.6 eV.

A nonlinear dependence on G and the presence in the solution of an exponential, Boltzmann-type term containing the energy E, is found also by the application of a purely diffusional scheme[22] under the same assumption of dominant bimolecular reactions, even if the details of such dependencies are slightly different.

As a consequence, we can conclude that the main point which determines the qualitatively most significant dependencies on experimental parameters of beam-induced SPE is the selection of the defect reaction mechanisms. In fact, under a similar assumption on this point, the application either of a diffusion- or of an interface-limited approach leads to differences in the results which are qualitatively less important.

To our knowledge, no explicit correlation of experimental results of EBIEC obtained at temperatures between 200 and 450 °C (Ref. 25) to the prediction expressed in Eq. (12), or to the model of Ref. 22, has been made. A qualitative agreement in temperature and dose rate dependence would suggest that the recombination mechanism depends on T and that also for EBIEC a picture in which direct mutual defect interactions dominate is more appropriate for $T \geq 200$ °C.

E. Effects of electronic stopping and under-threshold elastic collisions

It has been suggested (see, for instance Refs. 38 and 39) that electronic stopping may be the dominant mechanism of beam-induced crystallization in some compound materials, due to the existence of defect production mechanisms induced by electronic excitation alone.

The discussion about the occurrence of such mechanisms in Si has lasted many years (for a review on this subject see Ref. 40). The prevailing point of view is that electronic excitation cannot produce displacement damage in Si by itself. Nevertheless, it can influence the mobility (and, in general, the reactions) of already existing defects. Several different mechanisms of enhanced defect diffusion due to electronic excitations have been suggested (see, for instance Refs. 41 and 42).

The occurrence of EBIEC even at $T\simeq -258$ °C supports the existence of an irradiation-induced mechanism of mobility of defects, which, according to the results at thermal equilibrium, would otherwise be frozen.[43]

It may be expected that even if electronic effects play a role in IBIEC, this is probably hindered by the amorphizing effect of ions at the temperature for which such basically athermal effects could be identified. Nevertheless electronic effects have been supposed to influence the dynamics of damage accumulation and annealing in the surface region of MeV implanted Si,[5,44] where the ratio of electronic to nuclear stopping of ions increases, becoming more similar to the case of electron irradiation.

The examination of EBIEC results leads us to conclude that the defects produced by displacement collisions are necessary to promote EBIEC; electronic excitation can at most give an athermal component to their reaction rates.

It is interesting to note that a similar effect could, in principle, be attributed to elastic collisions which transfer energies lower than T_d.[42] The elastic cross section for transferred energies lower than about 3 eV *decreases* with increasing electron energy with a trend similar to the one shown by electronic stopping and opposite to the one shown by the displacement cross section σ_d (see Fig. 1). Figure 7 reports the elastic cross section for transferred

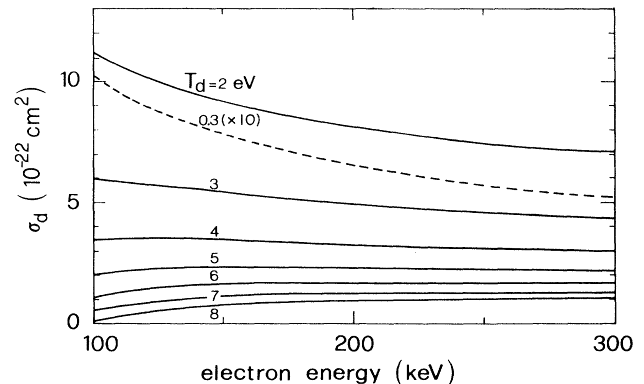

FIG. 7. Elastic cross section for transferred energies $T \geq T_{min}$ as a function of electron energy, for different values of the minimum transferred energy T_{min}. The scale for the dashed line, relative to $T_{min}=0.3$ eV, has to be multiplied by a factor of 10.

energies $T \geq T_{\min}$ as a function of electron energy, for different values of the minimum transferred energy $T_{\min}$. The dashed curve represents $T_{\min}=0.3$ eV, which is a typical value of energy necessary for defect migration.

The trends of the electronic and under-threshold elastic cross sections, compared with the displacement cross section σ_d, suggest that the reduction of the temperature dependence of EBIEC rate with decreasing electron energy could be qualitatively explained by the increasing amount of the athermal component of reaction energy available for each defect produced, as foreseen by both the above mechanisms.

V. CONCLUSIONS

The results of EBIEC, obtained in a TEM on cross sections of amorphous self-implanted Si layers at temperatures in the range $-258 \leq T \leq 20\,^{\circ}\mathrm{C}$ point out the following.

(i) The basic mechanism of the induced epitaxial crystallization is the production of defects by nuclear elastic collisions; inelastic stopping or elastic under-threshold effects alone cannot induce the transformation.

(ii) The rate of the transformation is very weakly dependent on temperature and always >0 (i.e., no transition to layer-to-layer amorphization is observed) in the range investigated. The apparent activation energies in the range $-170 \leq T \leq 20\,^{\circ}\mathrm{C}$ are 1–2 orders of magnitude lower than the typical migration energies of point defects in Si lattice; moreover the temperature dependence becomes still weaker in the range $-258 \leq T \leq -170\,^{\circ}\mathrm{C}$.

(iii) The thickness of the regrown layer per unit dose is independent of the beam current density and proportional to the cross section for elastic displacement, calculated by assuming a threshold energy in the range $12 \leq T_d \leq 14$ eV.

Some effects, such as the reduction of temperature dependence of EBIEC rate with decreasing electron energy, in connection with the results reported in point (ii), could be explained by the assumption that electronic stopping and/or under-threshold elastic collisions play a role in the process, supplying an athermal contribution to the reaction rates of the defects responsible for the transformation.

The comparison made with known results and published models of IBIEC has, first of all, underlined that many differences in the qualitative behaviors of IBIEC and EBIEC can be explained in a natural way by considering the trend in the data of IBIEC when decreasing ion mass and temperature. In fact, they show deviations from the models which fit the data of heavier ions, in a direction consistent with the results of EBIEC.

Even if no attempt has been made here to discriminate between the interface- or diffusion-limited character of IBIEC and EBIEC, nevertheless it is concluded that different assumptions about the basic defect reactions, probably related to the two different ranges of temperature in which the two processes have been characterized, are necessary to explain the results of IBIEC and EBIEC. While, in fact, the assumption of dominant direct mutual interactions seems essential to explain IBIEC results, a linear-recombination mechanism seems more appropriate for low-temperature EBIEC.

The capability of EBIEC to occur at very low temperatures, due to the ineffectualness of electrons to induce amorphization of Si, allows the observation of effects, hypothetically influenced by electronic excitation or by under-threshold elastic collisions, which are hindered in IBIEC due to the amorphization occurring at low T. Nevertheless, the observation of similar effects may be expected in the surface region of Si implanted with light ions at MeV energies, where the stopping characteristics of ions become more similar to those of electrons.

ACKNOWLEDGMENTS

Thanks are due to the personnel of Hitachi Ltd. for their careful assistance, and to F. Corticelli and A. Garulli for TEM specimen preparation. This work was partially supported by CNR–Progetto Finalizzato Materiali e Dispositivi per l'Elettronica allo Stato Solido.

[1]N. N. Gerasimenko, A. V. Dvurechenskii, G. A. Kachurin, N. B. Pridachin, and L. S. Smirnov, Fiz. Tekh. Poluprovodn. **6**, 1834 (1972) [Sov. Phys. Semicond. **6**, 1588 (1973)].

[2]M. D. Matthews and S. J. Ashby, Philos. Mag. **27**, 1313 (1973).

[3]G. Holmén, S. Peterström, A. Burén, and E. Bøgh, Radiat. Eff. **24**, 45 (1975).

[4]I. Golecki, G. E. Chapman, S. S. Lau, B. Y. Tsaur, and J. W. Mayer, Phys. Lett. **71A**, 267 (1979).

[5]J. Nakata, M. Takahashi, and K. Kajiyama, Jpn. J. Appl. Phys. **20**, 2211 (1981).

[6]J. Linnros, B. Svensson, and G. Holmén, Phys. Rev. B **30**, 3629 (1984).

[7]R. G. Elliman, S. T. Johnson, A. P. Pogany, and J. S. Williams, Nucl. Instrum. Methods B **7-8**, 310 (1985).

[8]J. Linros, G. Holmén, and B. Svensson, Phys. Rev. B **32**, 2770 (1985).

[9]G. Lulli, P. G. Merli, and M. Vittori Antisari, Phys. Rev. B **36**, 8038 (1987).

[10]J. S. Williams, R. G. Elliman, W. L. Brown, and T. E. Seidel, Phys. Rev. Lett. **55**, 1482 (1985).

[11]J. Linnros and G. Holmén, J. Appl. Phys. **59**, 1513 (1986).

[12]J. Linnros and G. Holmén, J. Appl. Phys. **62**, 4737 (1987).

[13]W. L. Brown, R. G. Elliman, R. V. Knoell, A. Leiberich, L. Linnros, D. M. Maher, and J. S. Williams, in *Microscopy of Semiconducting Materials 1987,* edited by A. G. Cullis and P. D. Augustus, Institute of Physics Conference Series (Institute of Physics, Bristol, 1987), p. 61.

[14]J. S. Williams, W. L. Brown, R. G. Elliman, R. V. Knoell, D. M. Maher, and T. E. Seidel, in *Ion Beam Processes in Advanced Electronic Materials and Device Technology,* edited by B. R. Appleton, F. H. Eisen, and T. W. Sigmon, MRS Symposia Proceedings No. 45 (Materials Research Society, Pittsburgh, 1985), p. 49.

[15]F. Priolo, A. La Ferla, and E. Rimini, J. Mater. Res. **3**, 1212 (1988).

[16]G. Lulli, P. G. Merli, and M. Vittori Antisari, in *Fundamen-*

tals of Beam-Solid Interactions and Transient Thermal Processing, edited by M. J. Aziz, L. E. Rehn, and B. Stritzker, MRS Symposia Proceedings No. 100 (Materials Research Society, Pittsburgh, 1988), p. 375.

[17]R. G. Elliman, J. S. Williams, W. L. Brown, A. Leiberich, D. M. Maher, and R. V. Knoell, Nucl. Instrum. Methods B **19/20**, 435 (1987).

[18]H. A. Atwater, C. V. Thompson, and H. I. Smith, J. Appl. Phys. **64**, 2337 (1988).

[19]T. K. Chaki, Philos. Mag. Lett. **59**, 223 (1989).

[20]K. A. Jackson, J. Mater. Res. **3**, 1218 (1988).

[21]F. Priolo, C. Spinella, and E. Rimini, Phys. Rev. B **41**, 5235 (1990).

[22]V. Heera, Phys. Status Solidi A **114**, 599 (1989).

[23]F. Priolo and E. Rimini, Mater. Sci. Rep. **5**, 319 (1991).

[24]F. Corticelli, G. Lulli, and P. G. Merli, Philos. Mag. Lett. **61**, 101 (1990).

[25]D. Hoehl, V. Heera, H. Bartsch, K. Wollschläger, W. Skorupa, and M. Voelskow, Phys. Status Solidi A **122**, K35 (1990).

[26]G. Lulli, P. G. Merli, A. Garulli, and M. Vittori Antisari, in *Surface Chemistry and Beam-Solid Interactions,* edited by H. Atwater, F. A. Houle, and D. Lowndes, MRS Symposia Proceedings No. 201 (Materials Research Society, Pittsburgh, 1991), p. 381.

[27]J. W. Corbett and J. C. Bourgoin, in *Point Defects in Solids,* edited by J. H. Crawford, Jr. and L. M. Slifkin (Plenum, New York, 1975), Vol. 2.

[28]W. A. McKinley and H. Feshbach, Phys. Rev. **74**, 1759 (1948).

[29]L. W. Hobbs, in *Quantitative Electron Microscopy,* edited by J. H. Chapman and A. J. Craven (University of Edinbourgh, Edinbourgh, England, 1983), p. 399.

[30]R. Sinclair, M. A. Parker, and K. B. Kim, Ultramicroscopy **23**, 383 (1987).

[31]L. A. Miller, D. K. Brice, A. K. Prinja, and S. T. Picraux, in *Defects in Materials,* edited by P. D. Bristowe, J. E. Epperson, J. E. Griffith, and Z. Liliental-Weber, MRS Symposia Proceedings No. 209 (Materials Research Society, Pittsburgh, 1991), p. 171.

[32]J. Narayan, D. Fathy, O. S. Oen, and O. W. Holland, J. Vac. Sci. Technol. A **2**, 1303 (1984).

[33]H. A. Atwater, C. V. Thompson, and H. J. Kim, Nucl. Instrum. Methods B **39**, 64 (1989).

[34]J. A. Van Vechten, Phys. Rev. B **10**, 1482 (1974).

[35]A. B. Danilin, and V. N. Mordkovich, Appl. Phys. Lett. **59**, 1570 (1991).

[36]C. Spinella, S. Lombardo, and S. U. Campisano, Phys. Rev. Lett. **66**, 1102 (1991).

[37]S. M. Hu, in *Atomic Diffusion in Semiconductors,* edited by D. Shaw (Plenum, London, 1973), p. 217.

[38]D. J. Ehrlich and D. J. Smith, Appl. Phys. Lett. **48**, 1751 (1986).

[39]N. Kobayashi, H. Kobayashi, H. Tanoue, N. Hayashi, and Y. Kumashiro, in *Beam-Solid Interactions: Physical Phenomena,* edited by J. A. Knapp, P. Borgensen, and R. A. Zuhr, MRS Symposia Proceedings No. 157 (Materials Research Society, Pittsburgh, 1990), p. 119.

[40]V. S. Vavilov, A. E. Kiv, and O. R. Niyazova, Phys. Status Solidi A **32**, 11 (1975).

[41]J. D. Weeks, J. C. Tully, and L. C. Kimerling, Phys. Rev. B **12**, 3286 (1975).

[42]J. C. Bourgoin and J. W. Corbett, Radiat. Eff. **36**, 157 (1978).

[43]J. Bourgoin and M. Lannoo, in *Point Defects in Semiconductors II,* edited by M. Cardona, Springer Series in Solid-State Sciences Vol. 35 (Springer-Verlag, Berlin, 1983).

[44]T. A. Belykh, A. L. Gorodishchensky, L. A. Kazak, V. E. Semyannikov, and A. R. Urmanov, Nucl. Instrum. Methods B **51**, 242 (1990).

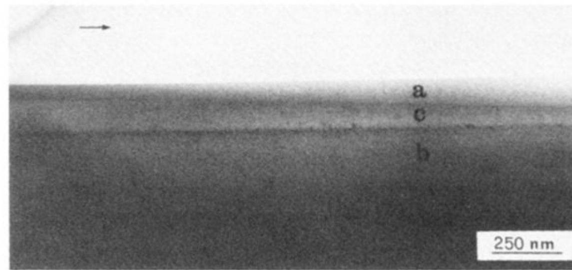

FIG. 2. TEM bright-field image of a cross section of self-implanted Si during heating *in situ* at 540 °C. The arrow indicates the direction along which the thickness of the specimen decreases. (a) amorphous layer, (c) epitaxially grown crystalline layer, (b) bulk crystal. The effect of the reduced SPE rate in the thinner region is evident.

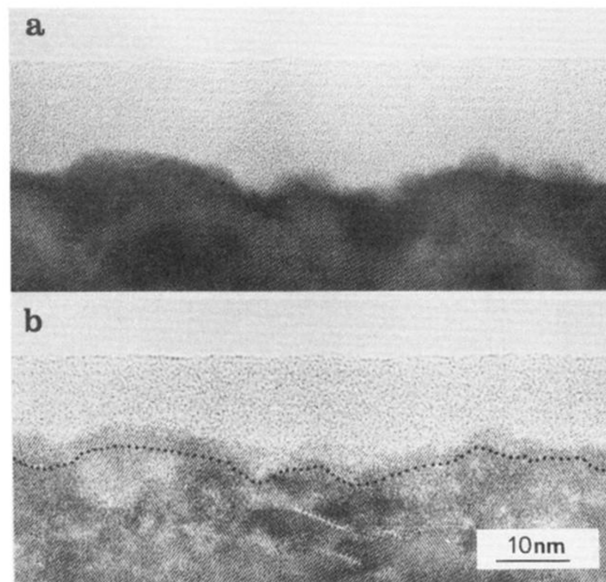

FIG. 6. High-resolution electron microscopy (HREM) image of a thin region of a self-implanted Si sample in (110) projection, before (a) and after (b) irradiation with 300-keV electrons for a time of 28 min at room temperature. The dotted line in (b) indicates the position of the original *a-c* interface.